Published OnlineFirst January 24, 2019; DOI: 10.1158/1940-6207.CAPR-18-0241

Research Article

Cancer Prevention Research

Sulforaphane Suppresses the Growth of Triple-negative Breast Cancer Stem-like Cells *In vitro* and *In vivo*

Nadia P. Castro[1], Maria C. Rangel[1], Anand S. Merchant[2], Gabriel MacKinnon[1], Frank Cuttitta[1], David S. Salomon[1], and Young S. Kim[3]

Abstract

Triple-negative breast cancer (TNBC) represents the poorest prognosis among all of breast cancer subtypes with no currently available effective therapy. In this study, we hypothesized that sulforaphane, a dietary component abundant in broccoli and its sprouts, can inhibit malignant cell proliferation and tumor sphere formation of cancer stem-like cells (CSC) in TNBC. CSC population was isolated using FACS analysis with the combined stem cell surface markers, $CD44^+/CD24^-/CD49f^+$. The effect of sulforaphane on a stem-related embryonic oncogene CRIPTO-1/TDGF1 (CR1) was evaluated via ELISA. *In vivo*, BalbC/nude mice were supplemented with sulforaphane before and after TNBC cell inoculation (daily intraperitoneal injection of 50 mg sulforaphane/kg for 5 and 3 weeks, respectively), and the effects of sulforaphane during mammary tumor initiation and growth were accessed with NanoString gene analysis. We found that sulforaphane can inhibit cell proliferation and mammosphere formation of CSCs in TNBC. Further analysis of gene expression in these TNBC tumor cells revealed that sulforaphane significantly decreases the expression of cancer-specific CR1, CRIPTO-3/TDGF1P3 (CR3, a homologue of CR1), and various stem cell markers including Nanog, aldehyde dehydrogenase 1A1 (ALDH1A1), Wnt3, and Notch4. Our results suggest that sulforaphane may control the malignant proliferation of CSCs in TNBC via Cripto-mediated pathway by either suppressing its expression and/or by inhibiting Cripto/Alk4 protein complex formation. Thus, the use of sulforaphane for chemoprevention of TNBC is plausible and warrants further clinical evaluation.

Introduction

Triple-negative breast cancer (TNBC) is characterized by a basal/mesenchymal phenotype that lacks estrogen receptor (ER), progesterone receptor (PR), and HER2/neu protein expression and represents a subtype of breast cancer associated with poor prognosis and highly aggressive behavior. Approximately 10%–20% of all breast carcinomas belong to this subtype of malignancy that is responsible for a much higher proportion of cancer mortality (1). Currently, no specific preventive or therapeutic agents for TNBC have been identified.

Cancer stem-like cells (CSC), also known as tumor-initiating cells, share several characteristics associated with normal tissue stem cells and have been identified in human tumors as possessing long-term self-renewal potential, quiescent properties, and resistance to chemotherapy and radiotherapy (2). CSCs were first identified in hematopoietic system malignancies and further characterized in solid tumors of breast, lung, prostate, colon, brain, head and neck, and pancreas (3). A putative breast CSC subpopulation can be isolated by FACS using several combinations of cell surface and noncell surface markers, followed by functional assays demonstrating their enriched tumorigenic potential (4). The first CSC subsets that were identified in breast tumors were cells possessing $CD44^+/CD24^-$ signatures and were recognized as prospective CSCs for both luminal and basal/mesenchymal human breast cancer cell lines, MCF-7 and MDA-MB-231, respectively (5). More recently, a study using 13 widely used stem/progenitor cell markers, individually or in combination, has demonstrated that both normal and malignant breast cells with the $CD44^+/CD24^-$ phenotype have the highest stem/progenitor cell capability when used in combination with Ep-CAM and CD49f reference markers (6). CSCs isolated with $CD44^+/CD24^-$ from $CD49f^+$

[1]Tumor Growth Factor Section, Mouse Cancer Genetics Program, NCI, Frederick, Maryland. [2]Center for Cancer Research Collaborative Bioinformatics Core, NCI, Bethesda, Maryland. [3]Nutritional Science Research Group, Division of Cancer Prevention, NCI, Rockville, Maryland.

Note: Supplementary data for this article are available at Cancer Prevention Research Online (http://cancerprevres.aacrjournals.org/).

Corresponding Author: Young S. Kim, NIH, MSC 9788,9609 Medical Center Dr., Rockville, MD 20892-9788. Phone: 240-276-7115; Fax: 240-276-7845; E-mail: kimyoung@mail.nih.gov

doi: 10.1158/1940-6207.CAPR-18-0241

Published OnlineFirst January 24, 2019; DOI: 10.1158/1940-6207.CAPR-18-0241

subpopulations formed more tumorspheres than those from $CD49f^-$ subpopulations, indicating that it is advantageous to use CD49f as a marker in combination with a $CD44^+/CD24^-$ pattern (6). Thus, the cell population of $CD44^+/CD24^-/CD49f^+$ was isolated and used in this study as a representative for breast CSC populations.

There are at least seven CRIPTO/TDGF genes in the human genome and only two of these, CR1 and CR3, have an intact open reading frame that can be translated into functional Cripto proteins. CR1 is an embryonic gene that encodes Cripto-1 protein, which acts as a coreceptor for various growth factors including a subset of TGFβ family members such as Nodal growth, and differentiation factors 1 and 3 (GDF 1/3), and GRP78 during early development mediating Smad-dependent (canonical) signaling (7). Likewise, evidence exists that the CR3-encoded protein, Cripto-3, can also activate the Smad-dependent canonical signaling pathway (8, 9). With extensive research on CR1, it is now known that the expression of this gene is significantly reduced in adults and confined to the stem cell compartment at specific tissues such as the colon, bone marrow, skin, and breast, although it can be fully reexpressed during malignant cell transformation in a number of different types of human tumors including TNBC (3). It is also known that CR1-encoded protein, Cripto-1, is an essential component in initiating and maintaining the expression of several pluripotent stem cell markers including Oct4 and Nanog (7, 10).

Cruciferous vegetables contain large amounts of glucoraphanin that are attributed to their cancer-preventive properties. These sulfur-rich compounds are hydrolyzed by the plant endogenous enzyme, myrosinase, to release an active compound, sulforaphane (11). Recently, sulforaphane has been shown to target the self-renewal properties of CSCs in a variety of cancer types including skin, breast, pancreatic, and glioblastoma (12–15). Despite the increasing evidence and interest shown in modulating effects of sulforaphane on CSCs and their involvement with the early development of tumor formation, limited data is available for the utility of sulforaphane to prevent the CSC-mediated processes of tumor development and maintenance. In this study, we have demonstrated that sulforaphane suppresses the self-renewal property of CSCs with high sensitivity, which may be involved with Cripto-related oncogenic signaling pathways in TNBC cells.

Materials and Methods

Cell lines and reagents

Human TNBC breast cancer MDA-MB-231-Luc-D3H1 cells were kindly provided by G. Charles Ostermeier (Leidos/Frederick National Laboratory for Cancer Research). The cells were grown in Eagle minimum essential medium (MEM; ATCC; Eagle MEM; catalog no. 30-2003) supplemented with 10% FBS and 2 mmol/L L-Glutamine. The MDA-MB-231-Luc-D3H1 cell line was derived from MDA-MB-231 human adenocarcinoma cells by stable transfection of the North American Firefly Luciferase gene expressed from the SV40 promoter (Caliper). The mouse mammary TNBC carcinoma cell line JygMC(A) cells were generously provided by Dr. Shogo Ehata (University of Tokyo, Tokyo, Japan). The cells were maintained in DMEM 1× (Gibco by Life Technologies), supplemented with 10% FBS and 100 U/mL penicillin, and 100 μg/mL streptomycin at 37°C in 5% CO_2. The JygMC(A) cells were transduced by a lentivirus promoter containing a fusion of firefly luciferase and eGFP reporters (pFUGW FerH ffLuc2 neo eGFP) as documented previously (16). R, S- sulforaphane was purchased from LKT Laboratories, Inc., dissolved in 0.9% NaCl solution, and stored at −20°C under N_2 gas.

Mouse strains and animal care

Animals used in this study were female Balb/C nude mice aged 6–9 weeks (Jackson Laboratory). AIN-96G–purified diet containing no sulforaphane (Harlan Teklad Inc.) was used to feed the animals. Animal procedures were conducted under conditions approved by the NCI at the Frederick Animal Care and Use Committee (ACUC) that follows the Public Health Service Policy for the Care and Use of Laboratory Animals outlined in the "Guide for Care and Use of Laboratory Animals". The NCI animal facility is approved by Assessment and Accreditation of Laboratory Animal Care International (AAALAC)

Orthotopic mammary fat pad injection and primary tumor formation

In vivo experiments were performed as previously reported by Castro and colleagues (16). For tumor growth experiments, 5×10^4 of MDA-MB-231-Luc-D3H1 cells were injected into the fourth mammary fat pads in both sides of 60 animals in three groups (20/group): control, pre- and posttreatment groups. Animals were treated with daily intraperitoneal injections of sulforaphane (50 mg/kg), whereas the control group received saline. The posttreatment group was injected with sulforaphane for 3 weeks after tumor cell transplantations into the fat pads, and the pretreatment group was pretreated with sulforaphane for 2 weeks before tumor cell injection and thus, a total of 5-week treatment with sulforaphane. Mammary primary tumors were collected at day 36 after cell implantation.

For the tumor-initiating capacity experiment, 5×10^4 of MDA-MB-231-Luc-D3H1 cells were injected into both fourth mammary fat pads of 10 animals (5 mice/group). The control and pretreated groups received saline or sulforaphane (50 mg/kg), respectively, for 2 weeks before cell injection. The treatment was continued for 3 additional weeks after the cell injection. Tumor growth was assessed and measured twice a week. Tumor volume was calculated using the formula, $^1/_2$ (L × W × D), where L = length,

Published OnlineFirst January 24, 2019; DOI: 10.1158/1940-6207.CAPR-18-0241

W = width, and D = depth. Mammary primary tumors were collected at day 20 after cell implantation.

Cell viability and proliferation assays

Sulforaphane effects on cellular viability were evaluated using the Countess automated cell counter (Invitrogen) to count cells based on Trypan blue dye exclusion after 52–54 hours of sulforaphane treatment. For proliferation assays, cells were seeded in 96-well dishes in quadruplicate at 5×10^3 cells/well and cultured for 48 hours in 5% FBS culture medium using the Vybrant MTT [3-(4,5-dimethylthiazol-2-yl)-2,5-diphenyltetrazolium bromide] Cell Proliferation Assay Kit in accordance to manufacturer instructions (Molecular Probes).

Tumorsphere-forming assay

Sphere formation assays were performed as described previously (17). In brief, cells were seeded in 24-well ultra-low attachment plates at 1×10^3 cells/well in 500 μL of MammoCult Human Medium Kit (catalog no. 05620, Stem Cell Technologies). Spheres were counted between 7–10 days after plating, using Gel Count TM—Oxford OPTRONIX version 1.03. To subculture the tumorspheres for secondary and tertiary generation, supernatant was removed and 1 mL of prewarmed Trypsin-EDTA (0.25%; StemCell Technologies) was used to dissociate the tumorspheres. Pellets were resuspended in MammoCult Human Medium and viable cells were counted according to the manufacturer's instructions. Similar cell densities were plated to form subsequent generations.

Flow cytometry

MDA-MB-231-luc-D3H1 cells were stained with the following antibodies: FITC rat anti-human CD49f, PE mouse anti-human CD44, Alexa Fluor 647 mouse anti-human CD24 (BD Pharmingen). Fluorescence-activated cell sorting BD, FACSAria II SORP, and FACSDiva 8.0.1 software were used. Stained cells were examined and sorted for stem/progenitor cells with $CD49f^+$ population followed by a final gate to select $CD44^+/CD24^-$ within the $CD49^+$ cell fraction. A total of 1.39×10^6 cells were sorted. The percentage of parent population were 98.31 of $CD49f^+$ marker, followed by a sequential gate of $CD24^+$ and $CD44^+$ with 0.01% and 1.30% of parental population, respectively. After sorting, cells were seeded in ultra-low adherent plates for tumorsphere-forming assays and treated with sulforaphane or control (0.9% NaCl) for 7–10 days.

RNA extraction protocol

All RNA tissue samples were snap-frozen in liquid nitrogen. Total RNA from tissue samples was extracted using TRIzol reagent according to the manufacturer's recommendations (Invitrogen). Total RNA from monolayer grown cells or tumorspheres was isolated and purified using the RNeasy Mini Kit (Qiagen) and subjected to DNAse treatment in accordance to manufacturer's instructions. Following extraction, 1 μg of total RNA was reverse transcribed using the RETROscript Kit (Ambion) in accordance with manufacturer's instructions.

NanoString analysis

Analysis was done using the NanoString nSolver2 application (Version 2.0.70). The Reporter Code Count files were imported along with the "gene panel" and Reporter Library File for the gene expression assay. As recommended, the raw digital count data processing steps included a subtraction of the background and negative codeset expression, followed by normalization against the positive codeset expression data. The normalized counts were then analyzed for their differential profile based on the group comparison: sulforaphane pretreatment versus saline control for tumor cells and normal cells, respectively. The table containing normalized counts, fold changes, and P values was exported as a spreadsheet. We used the Stem Cell nCounter (24 samples) and a Custom Gene Expression Assay nCounter (15) based on published literature of mRNA genes and controls classified as markers of embryonic stem cell, epithelial–mesenchymal transition (EMT), and mesenchymal–epithelial transition (MET) as reported previously (16). NanoString data in this publication have been deposited in NCBI's Gene Expression Omnibus (GEO) and are accessible through GEO Series accession number GSE80765.

Dual luciferase assay

MDA-MB-231-luc-D3H1 cells (7.5×10^4 cells/well in 24-well/plates) were transiently transfected with 0.5 μg of a human CR1 promoter luciferase reporter construct or the pGL3-enhancer luciferase empty vector using LipoD293 DNA *In Vitro* Transfection Reagent (Ver. II; SignaGen Laboratories). The pEF1α-*Renilla* control vector was cotransfected into all cells to normalize for transfection efficiency. Six to 8 hours after the transfection, serum-free medium containing either saline or sulforaphane (7.5 μmol/L; LKT Laboratories, Inc.) was added to wells. After 48 hours, the cells were lysed and luciferase activity was measured using the Dual-Luciferase Reporter Assay Kit (Promega) according to the manufacturer's instructions. All experiments were repeated three times with triplicate samples.

qRT-PCR

qRT-PCR reactions for 18 human genes that are relevant to stem or Cripto signaling pathways were performed in 16 samples (8 from control and 8 from sulforaphane pretreatment group) to validate the findings from the NanoString assay. The reactions were performed in the Mx3005P (Stratagene) with the Fast program using Brilliant Ultra-Fast SYBR Green QPCR MasterMix (Agilent Technologies) in a total volume of 20 μL. The list of genes and oligonucleotide sequences can be found in Supplementary

Published OnlineFirst January 24, 2019; DOI: 10.1158/1940-6207.CAPR-18-0241

Table S1. To evaluate the amplification of nonspecific products and primer-dimer formation, dissociation curves were analyzed. The reactions were performed in duplicate. The internal control gene, HPRT1 (GenBank: NM_000194.2), was considered in gene expression normalization. Relative gene expression between the sample groups was calculated using the Pfaffl model (18), employing the efficiency-corrected equation.

IHC staining and scoring

Formalin-fixed, paraffin-embedded mouse tissues were sectioned and processed as described previously (16). The IHC staining was estimated using the staining index (SI). The SI is the sum of the staining intensity and staining distribution. The slides were assessed for both the staining intensity and proportion of cells stained. The intensity was scored as 0 (no staining), 1 (weak), 2 (moderate), or 3 (strong). The distribution was scored as 0 (no staining), 1 (<10% of cells positive), 2 (11%–50% of cells positive), or 3 (>50% of cells positive). The two scores were added to give a final score of 0 to 6. A minimum of eight different areas per sample were analyzed under the microscope with 20× magnification.

ELISA studies

CR1 (R&D Systems, catalog no. 145-CR/CF), Nodal (R&D Systems, catalog no. 3218-ND-024/CF), GRP78 (Abcam, catalog no. ab78432), and Alk4 (Creative Bio-Mart, catalog no. ACVR1B-645H,) were purchased from the indicated vendors. CR1/BP interaction assays were run in parallel to that described previously by Klauzinska and colleagues (19). In brief, four different target proteins (Nodal, GRP78, ACVR1B/Alk4, and BSA) were solid phased to a 96-well plate (Costar, catalog no. 3591, Polystyrene) at 50 ng/50 μL/well in two separate columns containing octuplicate wells for each target protein, agitated for 2 hours on a rotary mixer and transferred to 4°C overnight. Then, half the target columns were exposed to 25 μL 1% BSA/PBS (negative control–100% CR1 binding), and the other half of the target columns were exposed to 25 μL sulforaphane (100 μmol/L). All the plates were treated with 25 μL CR1 (50 ng/well), 50 μL rabbit anti-N-terminal CR1 (Abcam, catalog no. ab103891), and 50 μL goat anti-rabbit IgG-HRP (Santa Cruz Biotechnology, catalog no. sc-2004) according to the procedure published previously (19). A PBS wash and 30-minute room temperature rotary shaker incubation was performed between each treatment following CR1 addition. Finally, stop solution (50 μL) was added to all wells and the plates were assessed for the absorbance at 450 nm on a CLARIOstar reader (BMG Labtech). Data was evaluated using Microsoft Excel program.

Statistical analysis

Statistical differences were determined using 2-tailed Student *t* test. Data are presented as mean ± SD.

Results

Sulforaphane inhibits proliferation of TNBC cells

Sulforaphane has previously been shown to inhibit the proliferation of skin and breast cancer cells (12, 13). We assessed the antiproliferative effects of sulforaphane using a mitochondrial activity test (MTT assay) in two TNBC cell lines: the mouse mammary carcinoma cell line, JygMC(A) GFP/Luc, and the human breast cancer cell line, MDA-MB-231-Luc-D3H1 (16, 20). Cells were treated with increasing concentrations of sulforaphane (0–20 μmol/L) for 48 hours. Viable cells in saline (control) and sulforaphane-treated groups were plotted (Fig. 1). The proliferation of these human and mouse TNBC cells was suppressed by 45% ($P < 0.001$) at 15 μmol/L sulforaphane for MDA-MB-231-Luc-D3H1 cells (Fig. 1A) and at 20 μmol/L sulforaphane for JygMC(A) GFP/Luc cells (Fig. 1B).

Sulforaphane inhibits the self-renewal of breast cancer stem/progenitor cells *in vitro*

To evaluate whether sulforaphane could reduce *in vitro* the stem cell–like self-renewal capacity of

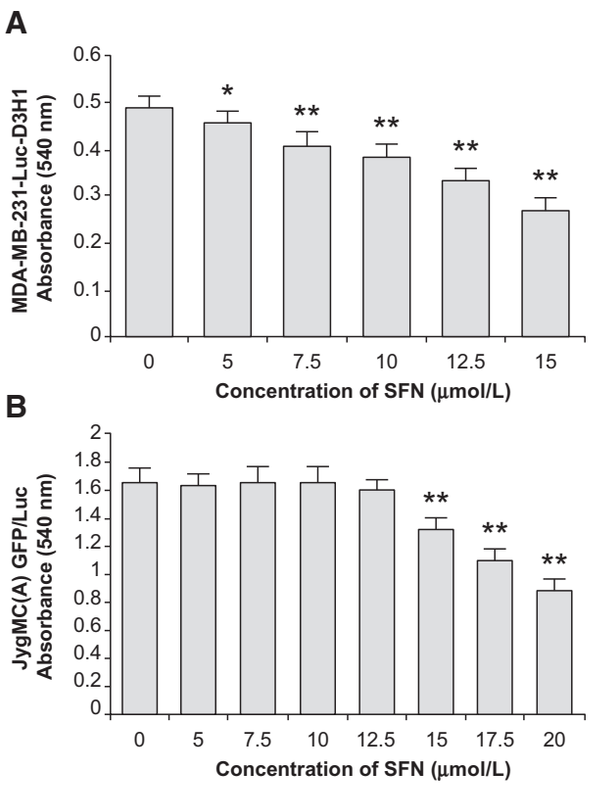

Figure 1.

In vitro growth-inhibitory effects of sulforaphane (SFN). Sulforaphane effects on human breast cancer cells (MDA-MB-231-Luc-D3H1; **A**) and mouse mammary cancer cells (JygMC(A) GFP/Luc; **B**) were measured by MTT assay. Data are representative of three experiments with quadruplicate samples. *, $P < 0.01$ and **, $P < 0.001$, as compared with control saline–treated cells (concentration of sulforaphane = 0).

Published OnlineFirst January 24, 2019; DOI: 10.1158/1940-6207.CAPR-18-0241

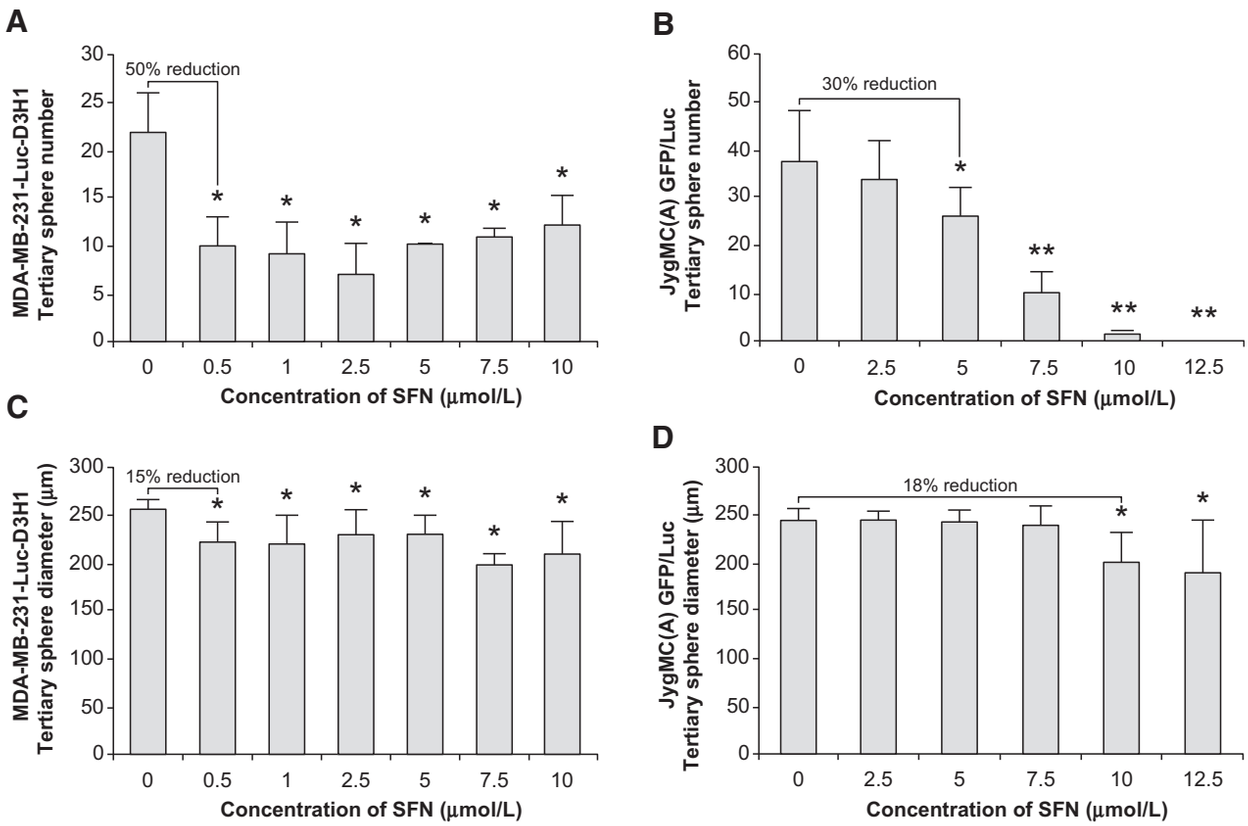

Figure 2.

Effects of sulforaphane on the mammospheres derived from TNBC cells. Average number and diameter of tertiary spheres in MDA-MB-231-Luc-D3H1 cells (**A** and **C**, respectively) and in JygMC(A) GFP/Luc cells (**B** and **D**, respectively). Data are representative of three experiments with quadruplicate samples. *, $P < 0.001$ and **, $P < 0.0001$, as compared with control saline-treated cells (concentration of sulforaphane = 0).

MDA-MB-231-Luc-D3H1 and JygMC(A) GFP/Luc TNBC cells, we seeded unsorted cell lines on ultra-low adherent plates without serum and growth factors and with varying concentrations of sulforaphane. Primary tumorspheres were generated within 10 days and then spheres were cultured for two additional passages in the presence or absence of sulforaphane. Sulforaphane decreased the number of tertiary tumorspheres by 50% with 0.5 μmol/L in MDA-MB-231-Luc-D3H1 cells (Fig. 2A) and 30% with 5 μmol/L in JygMC(A) GFP/Luc cells (Fig. 2B). Moreover, at the concentration of 12.5 μmol/L sulforaphane, the ability of JygMC(A) GFP/Luc cells to form tertiary tumorspheres was completely abolished by this dietary component (Fig. 2B).

Tertiary tumorsphere diameter was also reduced by 15% with 0.5 μmol/L sulforaphane in MDA-MB-231-Luc-D3H1 cells (Fig. 2C) and by 18% with 10 μmol/L sulforaphane for JygMC(A) GFP/Luc cells (Fig. 2D). It is interesting to note that a lower sulforaphane concentration (IC_{50} approximately 0.5 μmol/L for MDA-MB-231-Luc-D3H1 cells and 5 μmol/L JygMC(A) GFP/Luc cells) was able to suppress mammospheres formed in both human and mouse TNBC cells than those concentrations exhibiting antiproliferative effects shown in the MTT assay (IC_{50} approximately 5 μmol/L for MDA-MB-231-Luc-D3H1 cells and 15 μmol/L JygMC(A) GFP/Luc cells). These results indicate that the presumptive CSCs that form tumorspheres are more sensitive to sulforaphane treatment compared with the unsorted bulk of TNBC cells.

To ascertain whether sulforaphane could target human breast CSCs *in vitro*, we isolated the putative CSC populations from the MDA-MB-231-Luc-D3H1 cells using differential flow cytometry for segregation of cells with $CD49f^+$ and $CD24^-/CD44^+$ markers that represent potential breast cancer stem and/or progenitor cells (Fig. 3A; ref. 21). The sorting process is briefly explained in Materials and Methods under the subtitle of Flow cytometry. Sorted cells were plated on ultra-low adherent plates and treated with 7.5 μmol/L sulforaphane for 10 days. We chose to use this concentration of sulforaphane that is not toxic to cells yet is still effective in inhibiting proliferation and tumorsphere formation, a characteristic of CSCs that have been shown to be resistant to chemotherapy and radiotherapy (2). Treatment with

Published OnlineFirst January 24, 2019; DOI: 10.1158/1940-6207.CAPR-18-0241

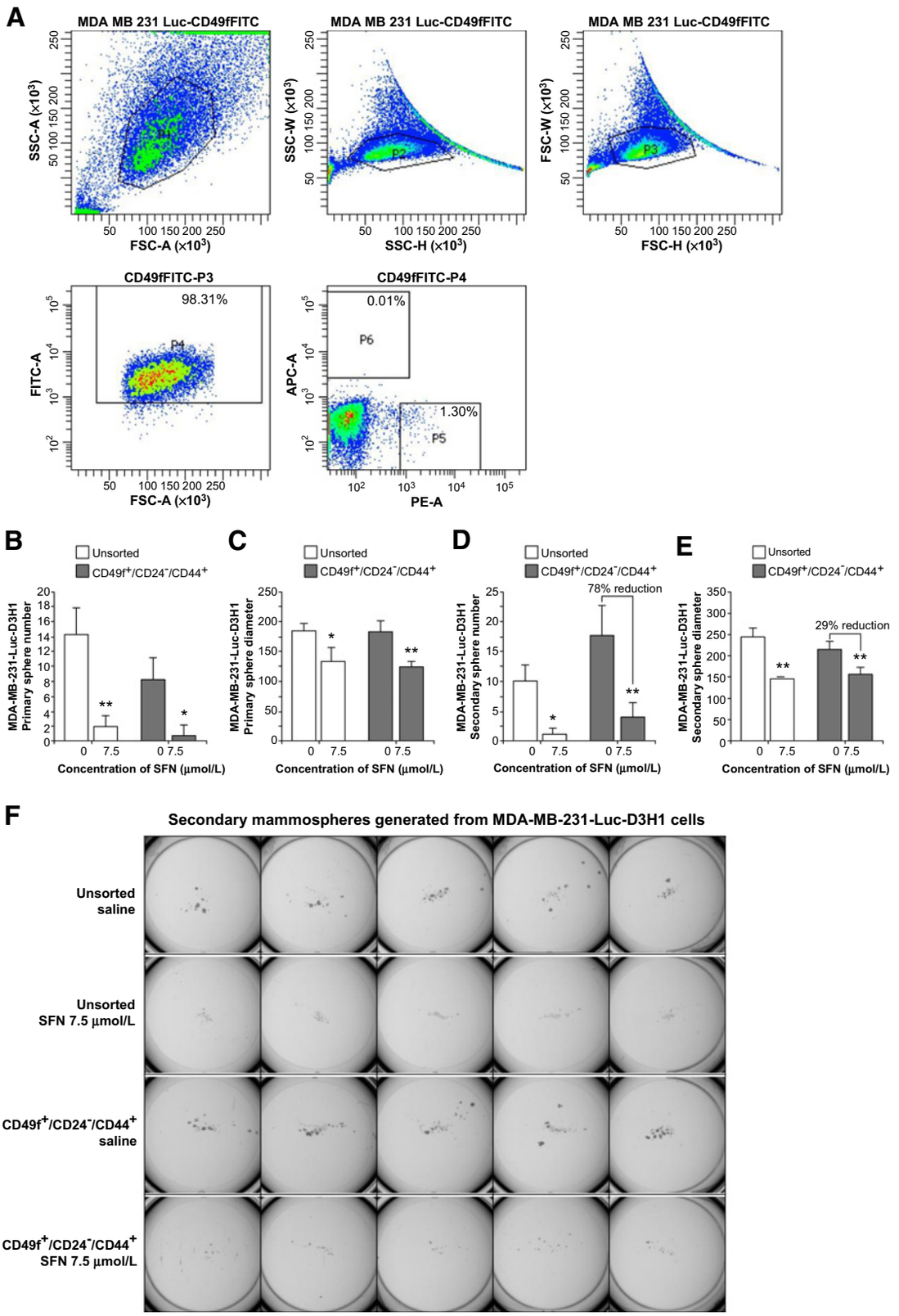

Published OnlineFirst January 24, 2019; DOI: 10.1158/1940-6207.CAPR-18-0241

sulforaphane produced a significant reduction in primary tumorspheres in number and diameter, compared with the untreated cells (Fig. 3B and C, respectively). We also noticed that the $CD49f^+/CD24^-/CD44^+$ subpopulation produced about twice the number of secondary tumorspheres when compared with unsorted cells (Fig. 3D), thereby confirming the increased self-renewal ability of this subpopulation. $CD49f^+/CD24^-/CD44^+$ cells treated with 7.5 μmol/L sulforaphane showed a significant reduction (78%) in secondary tumorsphere numbers when compared with the same subpopulation treated with saline (sulforaphane concentration = 0; Fig. 3D). Furthermore, the diameter of tumorspheres was also reduced in response to the treatment with 7.5 μmol/L sulforaphane (Fig. 3C and E). The effect of sulforaphane on the tertiary tumorspheres formed from the $CD49f^+/CD24^-/CD44^+$ subpopulation could not be examined due to the limitation of the number of available secondary tumorspheres. Finally, a representative photograph of the secondary tumorspheres in unsorted cells and in the $CD49f^+/CD24^-/CD44^+$ subpopulation, with or without 7.5 μmol/L sulforaphane treatment, is shown in Fig. 3F. These results clearly demonstrate that vegetable component sulforaphane effectively targets a drug-resistant CSC subpopulation in TNBC cells.

Sulforaphane inhibits tumor growth *in vivo*

To determine the potential *in vivo* effects of sulforaphane, we utilized a xenograft model of MDA-MB-231-Luc-D3H1 cells in female BalbC/nude mice of which 5×10^4 cells were transplanted orthotopically into mammary fat pads. The animals ($n = 60$) were treated with or without daily intraperitoneal injection of 50 mg sulforaphane/kg body weight (dose based on previous publications; refs. 22, 23). For the pretreated group, sulforaphane was given 2 weeks prior to tumor cell inoculation while it was provided simultaneously with the tumor cells for the posttreated group. Sulforaphane treatment was continued for 3 additional weeks after cell injection. Treatment was performed daily as 24 hours is the optimum time reported for complete elimination of sulforaphane from blood (24). Tumor cells were transplanted bilaterally into the fourth inguinal mammary fat pads. The suppressive effects of sulforaphane on mammary tumor formation reached a maximum at day 31 after tumor cell inoculation in the sulforaphane-pretreated group (Fig. 4A). At this time, mammary tumors in the sulforaphane pretreatment group ($n = 20$, 5 weeks) exhibited a 29% reduction in tumor volume, whereas it was approximately 50% less (14%) in the posttreatment group ($n = 20$, 3 weeks) as compared with control tumors (Fig. 4A). Sulforaphane treatment with this concentration had no apparent toxicity as indicated by no significant alterations in body weight (Fig. 4B).

Sulforaphane inhibits a gene expression profile of stem cell markers *in vivo* during primary tumor cell growth

To ascertain the potential effects of sulforaphane on the gene expression profile of stem cell markers during MDA-MB-231-Luc-D3H1 primary tumor cell growth, total RNA was extracted from the tumors obtained 36 days after the tumor cell injection. Two different NanoString nCounter Gene Expression Codesets were used to examine sulforaphane-induced changes in the gene expression. One was the Stem-Cell-Gene set, which is a commercially available standard panel of 193 stem cell markers plus 6 internal reference genes. The other consisted of a customized panel containing 102 embryonic stem cell markers and EMT and MET markers plus 5 internal reference genes (16). We built the latter NanoString platform based on published literature on CSC-related genes including CR1 and its homolog, CR3. The results from the NanoString mRNA analysis showed that sulforaphane inhibited the expression of a majority of the genes analyzed in both codesets. Specifically, with the commercially available panel, the expression of 95% of the genes were suppressed in the sulforaphane pretreatment group ($n = 10$) compared with the control-saline group ($n = 10$) during primary tumor cell growth. Forty-three of 193 genes, which include stem-related aldehyde dehydrogenase 1A1 (ALDH1A1) and NANOG, as well as a CR1-requiring growth factor, GDF3, and the embryonic pluripotency–maintaining transcription factor, Forkhead box D3 (FOXD3), showed a P value less than 0.05 and are listed in Supplementary Table S2. Of the nine genes that were upregulated with sulforaphane, only WNT11 came close to trending toward significance ($P = 0.079$) and its fold change was 1.26. With the customized codeset, 87% of the genes were down-regulated in the sulforaphane pretreatment group ($n = 12$) compared with the control saline group ($n = 12$). Thirty-three of 102 genes, which include cancer-specific CR1 and its homolog, CR3,

Figure 3.

Inhibitory effects of sulforaphane on mammospheres generated from MDA-MB-231-Luc-D3H1 cells. **A,** Representative plot showing the expression of each stem/progenitor cell marker in the gated $CD49f^+$ population as analyzed by flow cytometry. $CD44^+/CD24^-$ phenotype within $CD49f^+$ population enriches for basal progenitors in MDA-MB-231 cells. Percentage indicates positive parental population of stem/progenitor marker. P1: Forward scatter (FSC) × side scatter (SSC) area gate that identifies live cells of interest; P2: SSC height × SSC width; P3: FSC height × FSC width; P4: $CD49f^+$; P5: $CD44^+/CD24^-$; P6: $CD44^-/CD24^+$. Average of primary sphere number (**B**), diameter (**C**), secondary sphere number (**D**), and diameter (**E**). **F,** Representative pictures show sulforaphane treatment of secondary sphere formation. Average cell number and its SD per plate are as follows; unsorted saline: 9.8 ± 2.775, unsorted sulforaphane: 1 ± 1, $CD49f^+/CD24^-/CD44^+$ saline: 17.5 ± 5.19, $CD49f^+/CD24/CD44^+$ sulforaphane: 3.9 ± 2.47. Cells were seeded on 24-well ultra-low attachment plate in quintuplicate at 1×10^3 cells/well and cultured for 7–10 days. Data are representative of three experiments with quintuplicate samples. *, $P < 0.001$ and **, $P < 0.0001$ as compared with control saline-treated cells. Unsorted: unsorted MDA-MB-231-Luc-D3H1 cells; $CD49f^+/CD24^-/CD44^+$: CSCs FACS isolated using $CD49f^+/CD24^-/CD44^+$ biomarkers.

Published OnlineFirst January 24, 2019; DOI: 10.1158/1940-6207.CAPR-18-0241

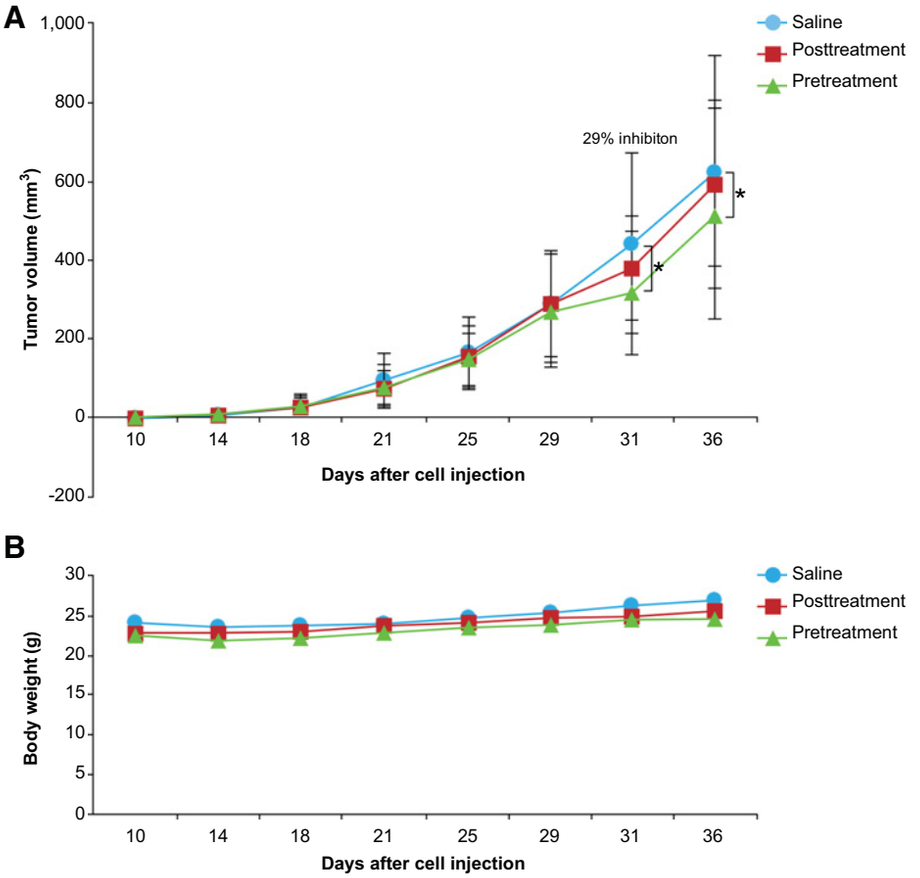

Figure 4.
In vivo effects of sulforaphane in MDA-MB-231-Luc-D3H1 xenograft mouse model. **A,** Sulforaphane-induced changes in tumor volume of BalbC/nude mice bearing mammary tumors. Twenty-nine percent inhibition was observed in sulforaphane-pretreated animals as compared with control saline-treated animals. *, $P < 0.001$. **B,** Body weight of the animals. All data are representative of 20 animals per group.

showed a P value less than 0.05 and are listed in Supplementary Table S3. Among the 13 genes that were upregulated, only TCF4 came close to trending toward significance ($P = 0.06$) and its fold change was 1.21. These analyses reveal that sulforaphane reduced the gene expression level of most stem cell markers *in vivo* during primary tumor growth when compared with animals treated with saline.

Sulforaphane's effects on gene expression of stem cell markers *in vivo* during early primary tumor initiation

Next, we decided to investigate the effects of sulforaphane on stem cell gene expression profiles during primary tumor initiation after only 20 days post cell injection, which was the time when a sufficient amount of tumor was available for RNA extraction needed for the same commercial and customized NanoString nCounter Gene Expression Codesets. Although there were trends that sulforaphane inhibited the expression of the majority of the genes analyzed in both codesets, none of the genes expressed during primary tumor initiation exhibited statistical significance ($P > 0.05$). These results suggest that the effect of sulforaphane on stem cell markers may be magnified during the tumor growth period and thus, the early detection for its efficacy seems to be limited.

qRT-PCR validation of differentially expressed genes as assessed by Nanostring analyses between sulforaphane pretreatment versus control

We selected 18 genes that are related to stem signaling pathway from the customized or commercial NanoString nCounter Gene Expression Codesets for further real-time mRNA validation. The NanoString-identified changes in the gene expression were confirmed using qRT-PCR in the sulforaphane pretreatment group ($n = 8$) paired with its control saline group ($n = 8$). The validated results in representative genes including CR1, FOXD3, WNT3, and NOTCH4 are shown in Fig. 5.

Sulforaphane reduces CR1 promoter activity

Next, we decided to further confirm the Nanostring-based evidence that CR1 gene expression is reduced by sulforaphane treatment. To ascertain this, we used a reporter system with a luciferase gene driven by the promoter for the human CR1 gene in the MDA-MB-231-Luc-D3H1 cells. The reporter can detect real-time CR1 promoter activity *in vitro*, which was validated in previously documented studies (25). Our results showed that sulforaphane was able to significantly reduce CR1 promoter activity *in vitro* by approximately 53% when compared with saline-treated cells (Supplementary Fig. S1).

Published OnlineFirst January 24, 2019; DOI: 10.1158/1940-6207.CAPR-18-0241

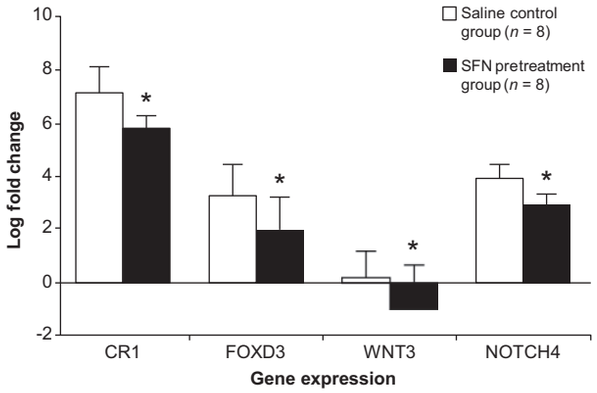

Figure 5.

Selected validation of NanoString gene expression analysis by qRT-PCR. Four genes including CR1, FOXD3, WNT3, and NOTCH4 are shown here as representatives for amplification. Data are the average of 8 samples from sulforaphane-pretreated group and 8 samples from saline control. All experiments were conducted in duplicates. *, $P < 0.05$ as compared with the control animals.

Protein expression of CR1 and CR3 is reduced in sulforaphane-pretreated primary tumor tissues

CR1 functions as an obligatory coreceptor for the TGFβ ligands, including Nodal and GDF3 (26). CR1 has also been shown to be involved in TNBC progression and, subsequently, lung metastasis (16). Thus, we selected CR1 to verify protein expression by IHC analysis in our model. Although this antibody and other commercially available antibodies cannot discriminate the five amino acid difference between CR1 and CR3, the stained Cripto proteins showed a lower level of expression in primary tumors obtained from sulforaphane-pretreated group when compared with those from the saline-treated control group (Fig. 6). These results suggest that sulforaphane not only suppresses the gene expression of CR1 and CR3 as shown in the analyses with NanoString but also their protein expression *in situ* as well.

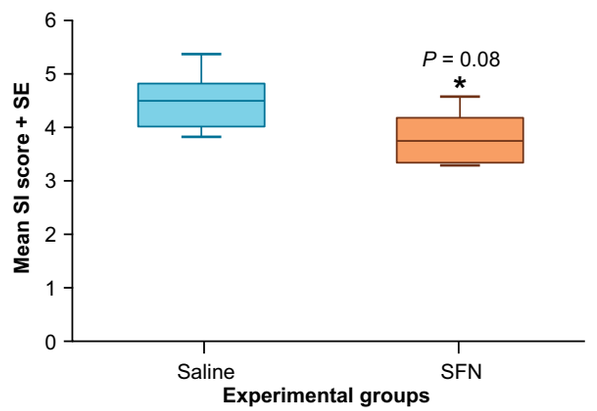

Figure 6.

Box plots for average SI scores evaluating IHC analysis of primary mammary tumors derived from MDA-MB-231-Luc-D3H1 xenografts for saline and sulforaphane groups. Each IHC staining was examined by two independent experts. The average SI scores for control and sulforaphane-treated groups were analyzed by *t* test [same as ANOVA in this case because there are two groups (sulforaphane-treated group and control) and two sets of SI scores]. The analysis resulted in a *P* value of 0.08 with a negative 1.3 fold change for SFN versus saline indicating that sulforaphane downregulated the oncoprotein Cripto expression by 30%. These results show that sulforaphane consistently downregulates Cripto protein expression *in vivo*. At least eight areas of 20× microscope fields were examined per sample.

Sulforaphane selectively inhibits CR1/BP interaction

Figure 7 is the graphic depiction of CR1 complex formation with solid-phased binding proteins (BP) including Nodal, GRP78, and Alk4 in the absence or presence of 100 μmol/L sulforaphane. Selective binding inhibition is clearly seen with sulforaphane showing progressive binding suppression for GRP78 (21% inhibition) and Alk4 (43% inhibition), while having little or no effect on Nodal. This data suggests that sulforaphane does not modify the binding of Nodal to its distinct binding site on CR1, which is the EGF-like domain (26), although sulforaphane suppressed the expression of Nodal and GDF3 in the NanoString mRNA analyses (Supplementary Table S3). Our data indicates that sulforaphane may interfere with the receptor complex that consists of CR1, Alk4, and GRP78, whereas it may indirectly suppress the expression of Nodal and GDF3 via an unclear mechanism(s). Overall, our study results suggest that sulforaphane possibly interrupts with the Cripto-mediated oncogenic pathway by specifically suppressing the ability of this protein to form a complex with its BPs including Alk4 and GRP78, but not Nodal.

Discussion

Patients with TNBC account for approximately 15%–20% of total breast cancer cases and possess a significant increase in the number of breast CSCs compared with those patients with non-TNBC (27). The enriched CSC population in TNBC may explain its distinct characteristics in drug resistance, frequent relapse, and distant metastases. This biologically aggressive form of breast cancer is associated with limited treatment options and poor patient prognosis. The median survival of advanced TNBC is 1 year, which is much shorter than that of other advanced breast cancer subtypes. Thus, there is an urgent need for the discovery of effective and nontoxic molecules that can block the development of this type of breast cancer.

Several studies have reported the efficacy of the cruciferous vegetable component, sulforaphane, in inhibiting CSCs in various organs including skin and breast (28, 29). Nevertheless, it has not been systematically demonstrated how this compound functions mechanistically in any specific tumor microenvironment in the context of ER (-), PR (-), and HER2/neu-negative TNBCs. To examine the effects of sulforaphane on this subtype of breast cancer that possesses an abundance of CSCs, we selected two different types of TNBC models, one derived from humans

Published OnlineFirst January 24, 2019; DOI: 10.1158/1940-6207.CAPR-18-0241

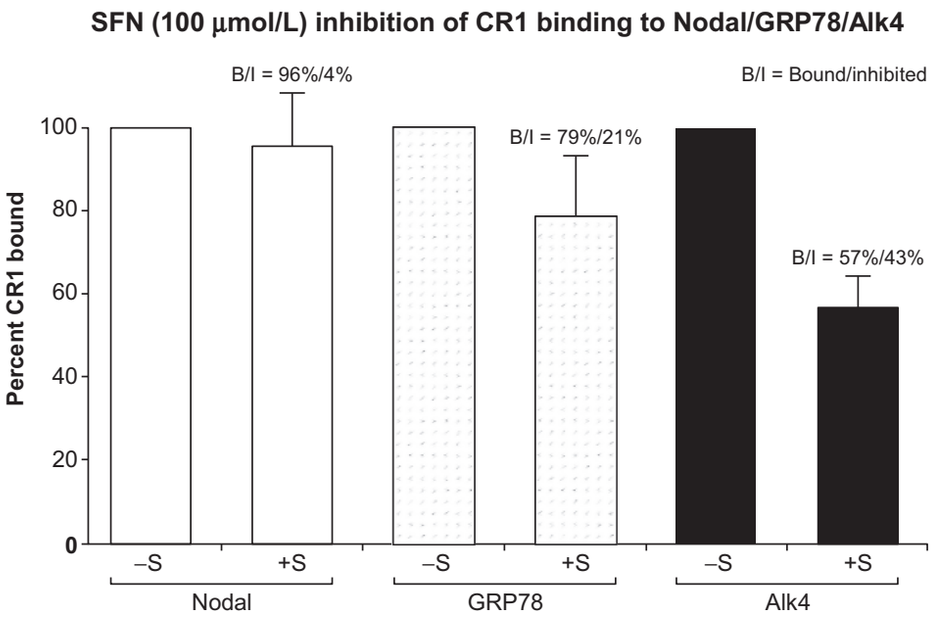

Figure 7.
ELISA assessment of CR1 binding to solid phase BPs including Nodal, GRP78, and Alk4 in the absence (−S) or presence (+S) of 100 μmol/L of sulforaphane. CR1 binding to individual BPs in the absence of sulforaphane (-S) condition was normalized to 100%. Percentage reaction–induced CR1 binding inhibition was then determined using the 100% reference point for respective BPs. Data represents average values determined from three separate studies with samples run in octuplicate.

(MDA-MB-231-Luc-D3H1) and the other from mice (JygMC(A) GFP/Luc; ref. 16). Interestingly, the JygMC(A) GFP/Luc cells contain an insertion of the mouse mammary tumor virus (MMTV) within the promotor of the Int3/Notch4 locus (30), which constitutively drives high expression of the oncogenic protein, Int3 and Notch4, and thereby maintains cancer stem-like phenotypes in these cells. Our data indicate that sulforaphane suppresses the proliferation of both human and mouse TNBC cells; however, the sensitivity to sulforaphane is higher in human MDA-MB-231-Luc-D3H1 cells than in mouse JygMC(A) GFP/Luc cells. The reason for this differential response remains unclear, but the existence of a strong endogenous viral promoter MMTV in the JygMC(A) GFP/Luc cells, which activates the Notch4 pathway that is intronic to breast CSCs (31), may provide these cells with the ability to be more resistant to sulforaphane treatment.

TNBC is also known to possess a rare subset of undifferentiated cells with embryonic stem-like characteristics within the tumor (32). This rare subpopulation is enriched with CSCs and progenitor cells which can be isolated and cultured as mammospheres based on their capability to self-renew and grow in suspension under anchorage-independent conditions. In this study, the primary mammospheres were cultured up to the third passage to make sure all the responding cells were either breast CSCs or progenitor cells. To evaluate the effects of sulforaphane on the mammosphere formation and maintenance, we isolated a CSC population from MDA-MB-231-Luc-D3H1 human cells using FACS analysis. When the cells containing $CD44^{+}/CD24^{-}/$ $CD49f^{+}$ were treated with natural vegetable constituent sulforaphane at a concentration of 7.5 μmol/L, they showed the significantly decreased property to form mammospheres *in vitro* (Fig. 3), indicating a reduced self-renewal capacity of these stem/progenitor cells.

To examine the effect of sulforaphane on tumor formation *in vivo*, BalbC/nude mice were supplemented with sulforaphane before and after MDA-MB-231-luc-D3H1 cell inoculation (daily intraperitoneal injection of 50 mg sulforaphane/kg for 5 and 3 weeks, respectively). Importantly, this dose used in *in vivo* treatment (5 mmol/L range) is several magnitudes higher than the dose used in *in vitro* ELISA studies (100 μmol/L sulforaphane). The suppressive effect of sulforaphane on the tumor volume was more pronounced when the treatment started before tumor implantation, yielding a 29% reduction for the sulforaphane-pretreated group ($n = 20$, 5 weeks) and a 14% reduction for the sulforaphane-posttreated group ($n = 20$, 3 weeks) compared with the respective controls ($n = 20$). Furthermore, the required concentration for the suppressive effects of sulforaphane against mammosphere formation was at least 2-fold lower than that for its antiproliferative properties, indicating the isolated CSCs in breast tumors are more sensitive to the sulforaphane treatment than the heterogeneous bulk of breast cancer cells. These results suggest that nontoxic dietary component sulforaphane could be used as a natural chemopreventive agent as it reduces breast CSCs in terms of both number and size.

Using NanoString analysis and qRT-PCR, we have demonstrated that the expression of CR1 and its related molecules such as FOXD3, Wnt3, and Notch4 that are involved with tumor progression is ameliorated by sulforaphane

Published OnlineFirst January 24, 2019; DOI: 10.1158/1940-6207.CAPR-18-0241

treatment (Fig. 5). CR1 is a coreceptor for Nodal, an embryonic morphogen that belongs to the TGFβ superfamily. Interestingly, the expression of CR1 in normal breast tissue is negligible, whereas the expression of CR1 in TNBC is significantly increased as compared with other breast cancer subtypes (33). Sulforaphane-induced reduction in the expression of Wnt3 and Notch4 may be biologically significant because these two molecules can positively regulate CR1 expression through either a canonical β-catenin/Tcf pathway or by enhancing the proteolytic processing of the intracellular domain of Notch (34, 35). Furthermore, effects of sulforaphane on the binding of CR1 to its BPs including Nodal, Alk4, and GRP78 were examined using an ELISA assay. DNA sequence of CR1-binding sites that consist of EGF-like and Cripto-FRL1-Cryptic domains remains conservative and thus same as that of CR3 (8, 9). As a consequence, both CR1 and CR3 could bind to the same ligands to transmit the extracellular signals to the nucleus. We have found that although sulforaphane does not block the interaction between CR1 and its ligand Nodal, sulforaphane does however suppress CR1 complex formation with both Alk4 and GRP78. These ELISA analyses have suggested that sulforaphane may have an alternative effect on CR1 tumor biology by blocking CR1/BPs complex formation and potentially suppressing the signal transduction pathways associated with such biological complexes.

In summary, our findings indicate that sulforaphane (50 mg/kg) suppresses mammary tumor development in a TNBC animal model, possibly by targeting a CSC population. Further gene analyses revealed that sulforaphane particularly decreased the expression of various stem cell markers including CR1 and its cancer-specific homolog, CR3. Finally, the collective results in this study suggest that the use of sulforaphane for chemoprevention of TNBC is plausible and warrants further clinical evaluation.

Conclusion

In vitro and *in vivo* studies reveal that sulforaphane may suppress the self-renewal properties of TNBC cells by targeting the Cripto-mediated oncogenic signaling pathway.

Disclosure of Potential Conflicts of Interest

No potential conflicts of interest were disclosed.

Authors' Contributions

Conception and design: N.P. Castro, D.S. Salomon, Y.S. Kim
Development of methodology: N.P. Castro, M.C. Rangel, F. Cuttitta, D.S. Salomon
Acquisition of data (provided animals, acquired and managed patients, provided facilities, etc.): N.P. Castro, M.C. Rangel
Analysis and interpretation of data (e.g., statistical analysis, biostatistics, computational analysis): N.P. Castro, M.C. Rangel, A.S. Merchant, G.M. MacKinnon, Y.S. Kim
Writing, review, and/or revision of the manuscript: N.P. Castro, A.S. Merchant, Y.S. Kim
Administrative, technical, or material support (i.e., reporting or organizing data, constructing databases): N.P. Castro, Y.S. Kim
Study supervision: D.S. Salomon, Y.S. Kim

Acknowledgments

All authors were employees of the NCI. This study was supported by the NCI through both Intramural (Tumor Growth Factor Section in the Center for Cancer Research) and Extramural programs (Nutritional Science Research Group in the Division of Cancer Prevention). We would like to thank G. Charles Ostermeier for kindly providing the human TNBC breast cancer MDA-MB-231-Luc-D3H1 cells. Our appreciation also goes to NCI Center for Cancer Research (CCR) staff members including Karen Saylor for expert animal technical support, Alyson Baker and Daniel Bertolette for their assistance in the laboratory, Dominic Esposito for the design of reporter constructs, and Steve Shema for NanoString technical support. Likewise, we would like to thank our colleagues working in Frederick CCR Flow Cytometry Core including Kathleen and Noer, Roberta Matthai, and Guity Mohammadi for their technical support. Finally, the authors would like to thank Cindy Clark and Alicia Livinski at the NIH Library Writing Center for manuscript editing assistance.

Acknowledgments

This work was supported by funds from the National Cancer Institute Intramural and Extramural Program.

The costs of publication of this article were defrayed in part by the payment of page charges. This article must therefore be hereby marked *advertisement* in accordance with 18 U.S.C. Section 1734 solely to indicate this fact.

Received July 2, 2018; revised November 20, 2018; accepted January 11, 2019; published first January 24, 2019.

References

1. Zhang J, Wang Y, Yin Q, Zhang W, Zhang T, Niu Y. An associated classification of triple negative breast cancer: the risk of relapse and the response to chemotherapy. Int J C Exp Pathol 2013;6:1380–91.
2. Kreso A, Dick JE. Evolution of the cancer stem cell model. Cell Stem Cell 2014;14:275–91.
3. Bianco C, Rangel MC, Castro NP, Nagaoka T, Rollman K, Gonzales M, et al. Role of Cripto-1 in stem cell maintenance and malignant progression. Am J Pathol 2010;177:532–40.
4. Wei W, Lewis MT. Identifying and targeting tumor-initiating cells in the treatment of breast cancer. Endocr Relat Cancer 2015;22:R135–55.
5. Al-Hajj M, Wicha MS, Benito-Hernandez A, Morrison SJ, Clarke MF. Prospective identification of tumorigenic breast cancer cells. Proc Natl Acad Sci U S A 2003;100:3983–8.
6. Ghebeh H, Sleiman GM, Manogaran PS, Al-Mazrou A, Barhoush E, Al-Mohanna FH, et al. Profiling of normal and malignant breast tissue show CD44high/CD24low phenotype as a predominant stem/progenitor marker when used in combination with Ep-CAM/CD49f markers. BMC Cancer 2013;13:289.
7. Strizzi L, Margaryan N, Gilgur A, Hardy K, Normanno N, Salomon DS, et al. The significance of a Cripto-1-positive subpopulation of human melanoma cells exhibiting stem cell-like characteristics. Cell Cycle 2013;12:1450–6.

8. Sun C, Orozco O, Olson DL, Choi E, Garber E, Tizard R, et al. CRIPTO3, a presumed pseudogene, is expressed in cancer. Biochem Biophys Res Commun 2008;377:215–20.
9. Hentschke M, Kurth I, Borgmeyer U, Hubner CA. Germ cell nuclear factor is a repressor of CRIPTO-1 and CRIPTO-3. J Biol Chem 2006;281:33497–504.
10. Chen L, Kasai T, Li Y, Sugii Y, Jin G, Okada M, et al. A model of cancer stem cells derived from mouse induced pluripotent stem cells. PLoS One 2012;7:e33544.
11. Higdon JV, Delage B, Williams DE, Dashwood RH. Cruciferous vegetables and human cancer risk: epidemiologic evidence and mechanistic basis. Pharmacol Res 2007;55:224–36.
12. Kerr C, Adhikary G, Grun D, George N, Eckert RL. Combination cisplatin and sulforaphane treatment reduces proliferation, invasion, and tumor formation in epidermal squamous cell carcinoma. Mol Carcinog 2018;57:3–11.
13. Burnett JP, Lim G, Li Y, Shah RB, Lim R, Paholak HJ, et al. Sulforaphane enhances the anticancer activity of taxanes against triple negative breast cancer by killing cancer stem cells. Cancer Lett 2017;394:52–64.
14. Li S-H, Fu J, Watkins DN, Srivastava RK, Shankar S. Sulforaphane regulates self-renewal of pancreatic cancer stem cells through the modulation of Sonic hedgehog–GLI pathway. Mol Cell Biochem 2012;373:217–27.
15. Bijangi-Vishehsaraei K, Reza Saadatzadeh M, Wang H, Nguyen A, Kamocka MM, Cai W, et al. Sulforaphane suppresses the growth of glioblastoma cells, glioblastoma stem cell–like spheroids, and tumor xenografts through multiple cell signaling pathways. J Neurosurg 2017;127:1219–30.
16. Castro NP, Fedorova-Abrams ND, Merchant AS, Rangel MC, Nagaoka T, Karasawa H, et al. Cripto-1 as a novel therapeutic target for triple negative breast cancer. Oncotarget 2015;6:11910–29.
17. Bianco C, Castro NP, Baraty C, Rollman K, Held N, Rangel MC, et al. Regulation of human Cripto-1 expression by nuclear receptors and DNA promoter methylation in human embryonal and breast cancer cells. J Cell Physiol 2013;228:1174–88.
18. Pfaffl MW. A new mathematical model for relative quantification in real-time RT-PCR. Nucleic Acids Res 2001;29:e45.
19. Klauzinska M, Bertolette D, Tippireddy S, Strizzi L, Gray PC, Gonzales M, et al. Cripto-1: an extracellular protein – connecting the sequestered biological dots. Connect Tissue Res 2015;56:364–80.
20. Chavez KJ, Garimella SV, Lipkowitz S. Triple negative breast cancer cell lines: one tool in the search for better treatment of triple negative breast cancer. Breast Dis 2010;32:35–48.
21. Duru N, Gernapudi R, Lo P-K, Yao Y, Wolfson B, Zhang Y, et al. Characterization of the $CD49f^{+}/CD44^{+}/CD24^{-}$ single-cell derived stem cell population in basal-like DCIS cells. Oncotarget 2016;7:47511–25.
22. Innamorato NG, Rojo AI, Garcia-Yague AJ, Yamamoto M, de Ceballos ML, Cuadrado A. The transcription factor Nrf2 is a therapeutic target against brain inflammation. J Immunol 2008;181:680–9.
23. Kanematsu S, Yoshizawa K, Uehara N, Miki H, Sasaki T, Kuro M, et al. Sulforaphane inhibits the growth of KPL-1 human breast cancer cells in vitro and suppresses the growth and metastasis of orthotopically transplanted KPL-1 cells in female athymic mice. Oncol Rep 2011;26:603–8.
24. Cornblatt BS, Ye L, Dinkova-Kostova AT, Erb M, Fahey JW, Singh NK, et al. Preclinical and clinical evaluation of sulforaphane for chemoprevention in the breast. Carcinogenesis 2007;28:1485–90.
25. Mancino M, Strizzi L, Wechselberger C, Watanabe K, Gonzales M, Hamada S, et al. Regulation of human Cripto-1 gene expression by TGF-beta1 and BMP-4 in embryonal and colon cancer cells. J Cell Physiol 2008;215:192–203.
26. Gray PC, Vale W. Cripto/GRP78 modulation of the TGF-β pathway in development and oncogenesis. FEBS Lett 2012;586:1836–45.
27. Idowu MO, Kmieciak M, Dumur C, Burton RS, Grimes MM, Powers CN, et al. CD44(+)/CD24(-/low) cancer stem/progenitor cells are more abundant in triple-negative invasive breast carcinoma phenotype and are associated with poor outcome. Hum Pathol 2012;43:364–73.
28. Fisher ML, Adhikary G, Grun D, Kaetzel DM, Eckert RL. The Ezh2 polycomb group protein drives an aggressive phenotype in melanoma cancer stem cells and is a target of diet derived sulforaphane. Mol Carcinog 2016;55:2024–36.
29. Li Q, Eades G, Yao Y, Zhang Y, Zhou Q. Characterization of a stem-like subpopulation in basal-like ductal carcinoma in situ (DCIS) lesions. J Biol Chem 2014;289:1303–12.
30. Raafat A, Lawson S, Bargo S, Klauzinska M, Strizzi L, Goldhar AS, et al. Rbpj conditional knockout reveals distinct functions of Notch4/Int3 in mammary gland development and tumorigenesis. Oncogene 2009;28:219–30.
31. Harrison H, Farnie G, Howell SJ, Rock RE, Stylianou S, Brennan KR, et al. Regulation of breast cancer stem cell activity by signaling through the Notch4 receptor. Cancer Res 2010;70:709–18.
32. Rangel MC, Bertolette D, Castro NP, Klauzinska M, Cuttitta F, Salomon DS. Developmental signaling pathways regulating mammary stem cells and contributing to the etiology of triple-negative breast cancer. Breast Cancer Res Treat 2016;156:211–26.
33. Strizzi L, Postovit L-M, Margaryan NV, Seftor EA, Abbott DE, Seftor REB, et al. Emerging roles of nodal and cripto-1: from embryogenesis to breast cancer progression. Breast Dis 2008;29:91–103.
34. Morkel M, Huelsken J, Wakamiya M, Ding J, van de Wetering M, Clevers H, et al. Beta-catenin regulates Cripto- and Wnt3-dependent gene expression programs in mouse axis and mesoderm formation. Development 2003;130:6283–94.
35. Klauzinska M, Castro NP, Rangel MC, Spike BT, Gray PC, Bertolette D, et al. The multifaceted role of the embryonic gene Cripto-1 in cancer, stem cells and epithelial-mesenchymal transition. Semin Cancer Biol 2014;29:51–8.

AACR American Association for Cancer Research

Cancer Prevention Research

Sulforaphane Suppresses the Growth of Triple-negative Breast Cancer Stem-like Cells *In vitro* and *In vivo*

Nadia P. Castro, Maria C. Rangel, Anand S. Merchant, et al.

Cancer Prev Res 2019;12:147-158. Published OnlineFirst January 24, 2019.